JOURNAL OF MATERIALS SCIENCE 35 (2000) 4385–4391

Fatigue of cement foams in axial compression

JONG-SHIN HUANG*, ZI-HERNG HUANG
Department of Civil Engineering, National Cheng Kung University, Tainan, 70101 Taiwan
E-mail: jshuang@mail.ncku.edu.tw

The theoretical expression for fatigue of cement foams in axial compression is derived using dimensional argument analysis. Bending model and Basquin law for describing the fatigue of individual cell struts are employed in calculating the number of cycles to failure of cement foams. It is found that the fatigue of cement foams in axial compression depends on cyclic stress range, relative density and the fatigue parameters of solid material from which they are made. A series of tests are conducted on the compressive fatigue of alumina cement foams for various relative densities and cyclic stress ranges. Experimental results are compared to theoretical modeling; the agreement is good.

1. Introduction

Cast-in-place cement foams with low thermal conductivity and good workability have been used widely in many applications such as thermal insulators for roof-deck systems and lining fills for tunnels. Pre-cast cement foams are typically used in sandwich structures because they are fire-resistant and inexpensive compared to polymeric foams. For example, prefabricated housing wall panels with a cement foam core and gypsum faces have been used for a number of years in construction. Lightweight cement foams used as load-bearing components or noise protectors in high-rising buildings and bridges, in general, are subjected to a fatigue loading due to fluctuations in stress (such as wind or earthquake), temperature, or moisture content. The fatigue of cement foams after some cycles of loading might lead to a catastrophic failure of the structures. The structural integrity, essential to the designer, is thus mainly controlled by the fatigue life of cement foams. Therefore, the fatigue of cement foams should be investigated in detail to provide ways of enhancing the safety of engineering structures.

Studies of the fatigue of foamed materials are limited in literatures. Noble and Lilley [1] obtained the fatigue macrocrack propagation rates for rigid polyurethane foams at room temperature under a constant cyclic loading. The fatigue of rigid polyurethane foams was described well by a modified form of Paris law. Yau and Mayer [2] studied the fatigue resistance of glass-reinforced rigid polycarbonate foams. Fatigue striation formed in the solid cell struts on fracture surface was observed, suggesting that the fatigue of solid cell struts is the main mechanism for the fatigue of foamed materials. Tsai and Ansell [3] measured the flexural fatigue properties of various woods, foam-like materials, and found that cell strut kinking is the main mechanism for flexural fatigue of their wood specimens. Bonfield and Ansell [4] presented the fatigue properties of laminated wood. There was no specimen size effect on the fatigue life for their wood laminates under compression and shear.

Huang and Lin [5] derived the theoretical expressions of high cycle fatigue, low cycle fatigue and macrocrack propagation rate for low relative-density foams with a critical macrocrack by using a cell-strut-bending model proposed by Gibson and Ashby [6]. Theoretical results suggested that the fatigue of low relative-density foams depends on relative density, cyclic stress intensity range and the fatigue parameters of solid materials from which they are made. By introducing preformed air bubbles into cement slurry and then mixing, Tonyan and Gibson [7] produced cement foams with relative densities in the range 0.1–0.45. The measured elastic moduli and compressive strengths of cement foams were analyzed by using both the cell-strut-bending model for foams and empirical equations for porous solids. Burman and Zenkert [8, 9] performed fatigue tests in four-point bending on sandwich beams with or without sub-surface core damage. Standard S-N diagrams and a Weibull type function were used to describe their fatigue test results on sandwich beams with two different polymeric foam cores, PVC and PMI.

In most cases, cement foams used in engineering structures, for instance tunnels and buildings, are subjected to a compressive stress state. The fatigue behavior of cement foams in axial compression becomes important when they are subjected to a cyclic mechanical or thermal loading. In the paper, the theoretical expression of compressive fatigue for cement foams without any critical macrocrack is first derived using dimensional argument analysis. Normally, the maximum cyclic compressive stresses imposed on cement foams are lower than their ultimate compressive strength. It is thus assumed that the fatigue of solid cement paste

* Author to whom all correspondence should be addressed.

follows Basquin law. Fatigue failure of cement foams occurs when individual cell struts within them rupture after some cycles of loading, giving the fatigue life of cement foams. As initial phase of study, cement foams under cyclic compressive stress ranges with zero stress ratios will be modelled and experimentally verified here.

2. Modeling

Fig. 1a shows cement foam cylinder subjected to a remote uniform cyclic compressive stress range, $\Delta\sigma^*$. The induced cyclic force, ΔF, exerted on individual cell struts with a cell strut length, ℓ, and a cell strut thickness, t, is shown in Fig. 1b. The minimum remote compressive stress $\sigma^*_{\min} = 0$, the maximum remote compressive stress $\sigma^*_{\max} = -\Delta\sigma^*$, the remote stress ratio $R = \sigma^*_{\min}/\sigma^*_{\max} = 0$ and the remote stress amplitude $\sigma^*_a = \Delta\sigma^*/2$ of the cement foam cylinder during each cycle of loading are illustrated in Fig. 2. Since cell-strut bending dominates the deformation of foamed materials, the cell-strut bending model of individual cell struts in cooperation with dimensional arguments analysis will be employed to derive the theoretical expression of compressive fatigue for cement foams.

The remote cyclic stress range imposed on the cement foam cylinder is related to the induced cyclic force exerted on individual solid cell-struts by using dimensional argument:

$$\Delta F \propto \Delta\sigma^* \ell^2 \tag{1}$$

The corresponding cyclic bending moment, ΔM, exerted on any cross-section of individual cell struts is proportional to the product of ΔF and ℓ. Thus, the induced cyclic stress range, $\Delta\sigma_s$, acting at any point of individual cell struts can be computed from the elementary mechanics of materials and dimensional argument analysis:

$$\Delta\sigma_s \propto \frac{\Delta M}{t^3} \propto \frac{\ell \Delta F}{t^3} \propto \Delta\sigma^* \left(\frac{\ell}{t}\right)^3 \tag{2}$$

The cross-section of individual cell struts is assumed to be square with an area of t^2.

The maximum remote compressive stress imposed on cement foams during each cycle of loading, in general, are lower than their ultimate compressive strengths in many engineering applications. As a result, the maximum induced cyclic stresses acting at individual cell struts are less than their modulus of rupture. Assuming that the fatigue of solid cement cell-struts can be described well by Basquin law:

$$\Delta\sigma_s (N_f)^a = C_1 \tag{3}$$

Where N_f is the number of cycles to failure, C_1 and a are the fatigue parameters of the solid from which cement foams are made.

Fatigue failure of cement foams occurs after some cycles of loading due to the fatigue failure of one set of solid cell-struts loaded cyclically up to their fatigue life. That is, the number of cycles to failure for cement foams, N^*_f, is equal to that for solid cement cell-struts, N_f. Hence, from Equations 2 and 3 the theoretical expression of the number of cycles to failure for cement foams can be found to be:

$$N^*_f = N_f \propto \left(\frac{1}{\Delta\sigma_s}\right)^{1/a} \propto \left[\frac{1}{\Delta\sigma^*}\left(\frac{t}{\ell}\right)^3\right]^{1/a} \tag{4}$$

The relative density of cement foams ρ^*/ρ_s (the density of cement foams, ρ^*, divided by the density of solid cements, ρ_s) is proportional to the ratio of t and ℓ. Hence, the compressive fatigue of cement foams can be written as:

$$\Delta\sigma^* (N^*_f)^a = g_0 \left(\frac{\rho^*}{\rho_s}\right)^{\alpha} \tag{5}$$

Here g_0 and α, the microstructure coefficients, depend on the cell geometry of cement foams and should be determined experimentally. Noted that the theoretical expression of compressive fatigue for cement foams (Equation 5) has a similar form as that for the solid cement from which they are made (Equation 3); both equations have the same exponential constant, namely a.

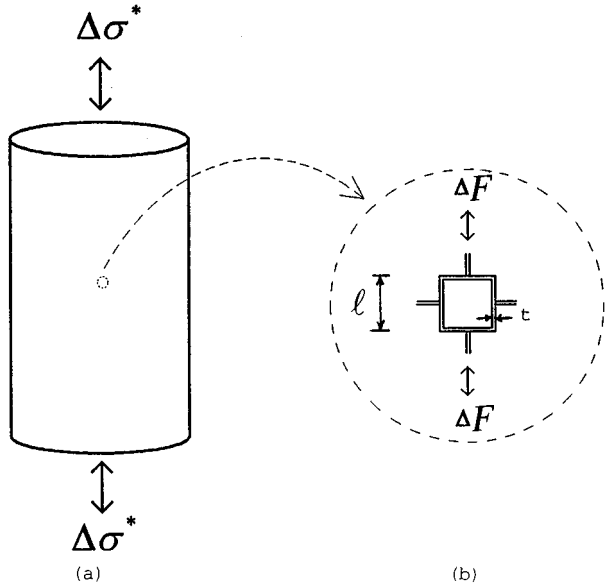

Figure 1 (a) Cement foam cylinder subjected to a remote uniform cyclic compressive stress range, $\Delta\sigma^*$. (b) The induced cyclic force range, ΔF, exerted on individual cell struts with a cell strut length, ℓ, and a cell strut thickness, t.

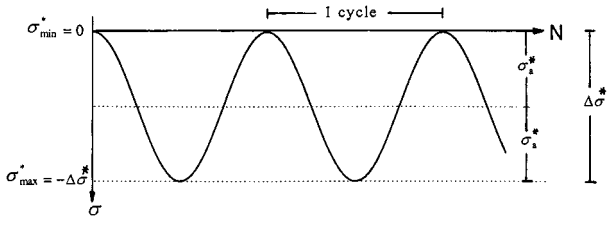

Figure 2 The minimum remote compressive stress $\sigma^*_{\min} = 0$, the maximum remote compressive stress $\sigma^*_{\max} = \Delta\sigma^*$, the stress ratio $R = 0$ and the stress amplitude $\sigma^*_a = \Delta\sigma^*/2$ during each cycle of loading.

Equation 5 has the limit that the number of cycles to failure N_f^* must equal to 1 when the maximum remote compressive stress exceeds the ultimate compressive strength of cement foams. As a result of that, Equation 5 is further reduced to an equation describing the relation between the ultimate compressive strength of cement foams and their relative density:

$$\sigma_u^* = g_0 \left(\frac{\rho^*}{\rho_s} \right)^{\alpha} \tag{6}$$

Substituting Equation 6 into 5, the theoretical expression of compressive fatigue for cement foams can be expressed in terms of their ultimate compressive strength:

$$\frac{\Delta\sigma^*}{\sigma_u^*} \left(N_f^* \right)^a = 1 \tag{7}$$

The analytical result indicates that once the compressive fatigue of any particular relative-density cement foams is known, the fatigue life of other relative-density cement foams can be estimated from Equation 7.

3. Experimental methods

3.1. Materials

A chemical processing method can produce cement foams; for example, aluminum powders are mixed with cement slurry to obtain an aerated cement paste within which hydrogen gas bubbles distribute randomly and uniformly. At the same time, a mechanical processing method by mixing preformed air bubbles with cement slurry can also be utilized to produce cement foams. All cement foam specimens tested in the study were made by the mechanical processing method; the mixing process and constituent proportion for producing cement foam specimens followed those as suggested by Tonyan and Gibson [7]. The materials used for producing cement foam specimens were alumina cement (Denka cement, Japan), water, superplasticizer and preformed air bubbles. The preformed air bubbles were made by pressurizing an aqueous solution of a foaming agent (manufactured by Elastizell Corporation of America, Ann Arbor, Michigan, U.S.A.) diluted with water in a foam generating tank. Cement foams with a water/cement ratio of 0.6 and adequate amounts of superplasticizer were made to ensure a good workability for placing them into cylindrical steel moulds. The dosage of superplasticizer (0.5% of total cement weight) is the same as that recommended [7] to reduce the water/cement ratio of the mix while maintaining a stable foam.

The design relative densities of cement foam specimens considered here were 0.15, 0.25 and 0.35; one solid cement specimen was also made. Changing the amount of preformed air bubbles poured into cement slurry controlled the density of cement foam specimens. The required amount of individual constituents for producing cement foam specimens with different densities was calculated and weighted before mixing. After complete mixing of cement paste and preformed air bubbles, cement foams were placed into cylindrical steel moulds with an inner diameter of 75 mm and a height of 150 mm. One day later, the cement foam specimens were removed from cylindrical steel moulds and cured at ambient room temperature in water. After 28 days of hardening, the cement foam specimens were trimmed on their both ends and then air dried for additional 7 days. Some cement foam specimens with imperfections such as visible cracks and flaws were observed and thus discarded. The actual density of each cement foam specimen was measured before mechanical testing.

3.2. Compression tests

For each design density of cement foams, 30 specimens were used for measuring the elastic modulus and ultimate compressive strength in uniaxial static compression tests at a constant strain rate of 0.001 min^{-1}. The loading frequency for wind and earthquake normally ranges from several to 25 Hz. Uniaxial dynamic compression tests on cement foam specimens were conducted under various remote cyclic stress ranges at a constant frequency of 20 Hz when both the consumption of testing time and the applicability of experimental results were of concern. The specimen numbers were 25, 32 and 45 for the design relative densities are 0.15, 0.25 and 0.35, respectively. In dynamic compression tests, the maximum remote compressive stress was less than the ultimate compressive strength of cement foams while the minimum remote compressive stress was zeroing during each cyclic loading as shown in Fig. 2. The number of cycles for each specimen is counted until failure occurs at which the remote cyclic compressive stress range can not be sustained. The maximum number of cycles allowable in dynamic compression tests was set to be 10^6; if specimens after 10^6 cycles of loading still kept intact, the dynamic compression test was stopped then. Both the static and dynamic compression tests were conducted in a materials testing machine (Instron Model 8511) with a 20 KN loading capacity.

4. Results and discussion

The average measured relative densities, ρ^*/ρ_s, are 0.141 with a standard deviation of 0.004, 0.266 with a standard deviation of 0.013 and 0.378 with a standard deviation of 0.007 for cement foam specimens with the design relative density of 0.15, 0.25 and 0.35, respectively. The measured density of solid cement specimen is $\rho_s = 1600$ kg/m^3. Air bubbles within cement foams are deformed under a loading of heavier cement paste as the design relative-density is increased, causing individual cells to collapse and coalesce before a complete hardening. As a result, the measured relative density is higher than the design relative density for cement foams with the design relative-density of 0.25 and 0.35.

4.1. Static compression test

In uniaxial static compression tests, two typical stress-strain curves for cement foam specimens were observed

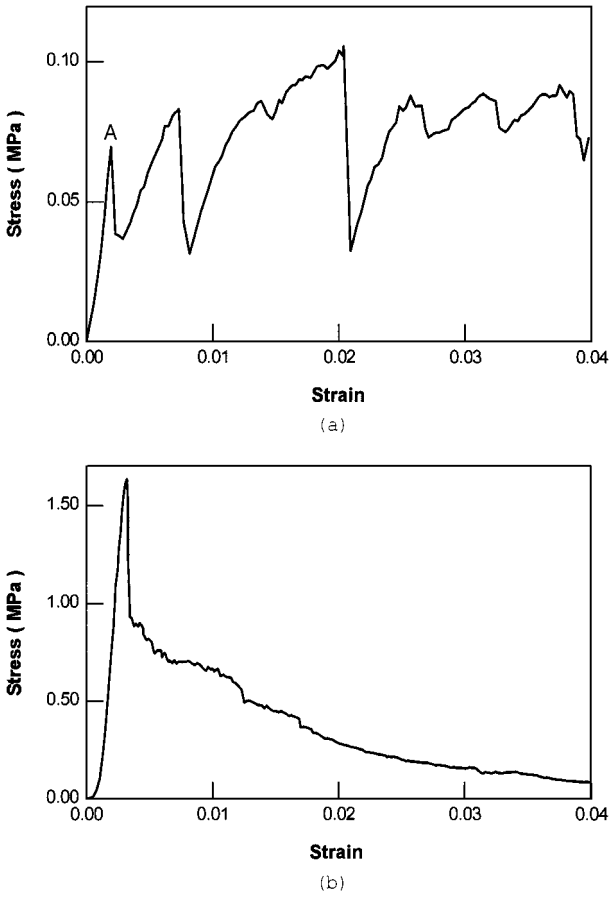

Figure 3 Two typical stress-strain curves for cement foam specimens in uniaxial static compression test (a) compressive crushing failure (b) shearing failure.

and illustrated in Fig. 3. Two different failure modes for cement foam specimens were also seen and shown in Fig. 4. A compressive crushing failure corresponding to the stress-strain curve in Fig. 3a occurs for cement foam specimens with the average relative density of 0.141 while a shearing failure corresponding to the stress-strain curve in Fig. 3b for those with the average relative density of 0.378. For cement foams with the average relative density of 0.266, both failure modes are found. Noted that brittle crushing of cell-struts is more likely to occur for lower relative-density cement foams with thinner cell-struts. When the applied stress reaches the first peak stress (labeled A in Fig. 3a), consecutive collapse of cell-struts progresses at a roughly constant stress, leading to the stress-strain curve as presented in Fig. 3a. For cement foams with higher relative densities, the cell struts become thicker enough to suppress the compressive crushing failure, exhibiting a shearing failure as expected for porous solids. Therefore, it can be said that the failure mode of cement foams will change from compressive crushing to shearing if their relative densities are larger than roughly 0.25.

The elastic modulus is measured from the slope of initial linear region of the stress-strain curve for each specimen while the ultimate compressive strength is calculated from the first peak load applied to the specimen as labeled A in Fig. 3. The measured elastic moduli of cement foams are plotted against their relative densities in Fig. 5. The relation between elastic modulus and relative density can be describe well by the following equation:

$$E^* = 21\left(\frac{\rho^*}{\rho_s}\right)^{3.2} \tag{8}$$

Here E^* has a unit of GPa. The exponential constant is found to be 3.2 instead of 2 as suggested by Gibson and Ashby [6] for low relative-density foamed materials.

Experimental results on the ultimate compressive strengths of cement foams with different relative densities are shown in Fig. 6. It is seen that the ultimate compressive strength of cement foams increases with their relative density and can be described well by the following equation:

$$\sigma_u^* = 120\left(\frac{\rho^*}{\rho_s}\right)^{3.6} \tag{9}$$

Here σ_u^* has a unit of MPa. The microstructure coefficient $g_0 = 120$ MPa is determined from the above equation. The exponential constant for relative-density dependence $\alpha = 3.6$, is within the range of 1.5 for low relative-density foams proposed by Gibson and Ashby [6] and 4.0 for porous solids suggested by Roy and Gouda [10].

4.2. Dynamic compression test

Experimental results on the numbers of cycles to failure for cement foam specimens with the average relative density of 0.141, 0.266 and 0.378 subjected to various cyclic compressive stress ranges are plotted in Figs 7–9, respectively. For specimens after 10^6 cycles of loading are still intact, their numbers of cycles to failure are set to be 10^6 as presented in the Figures. It is noted that the numbers of cycles to failure for cement foams with the average relative density of 0.141 scatter more widely. The reason might be due to the difficulty in controlling the microstructural uniformity when more preformed air bubbles are mixed with cement slurry for lower relative-density cement foams. Some specimens with a non-uniform microstructure might fail after few cycles of loading, resulting in a local collapse of thinner cell-struts and a shorter fatigue life as expected. From Fig. 7, however, it still can be seen that the numbers of cycles to failure increase with decreasing cyclic compressive stress ranges.

From Equation 5, it is clear that the numbers of cycles to failure for cement foams will be affected by their relative density and the cyclic compressive stress ranges. When the relative densities of cement foams are taken into account, the normalized cyclic compressive stress range, $\Delta\sigma^*/(\rho^*/\rho_s)^{3.6}$, are plotted against their corresponding numbers of cycles to failure for cement foams with various relative densities and are shown in Fig. 10. The relation between the number of cycles to failure and the normalized cyclic compressive stress range is found to be:

$$\left[\frac{\Delta\sigma^*}{(\rho^*/\rho)^{3.6}}\right] N_f^{*\,0.034} = 118 \tag{10}$$

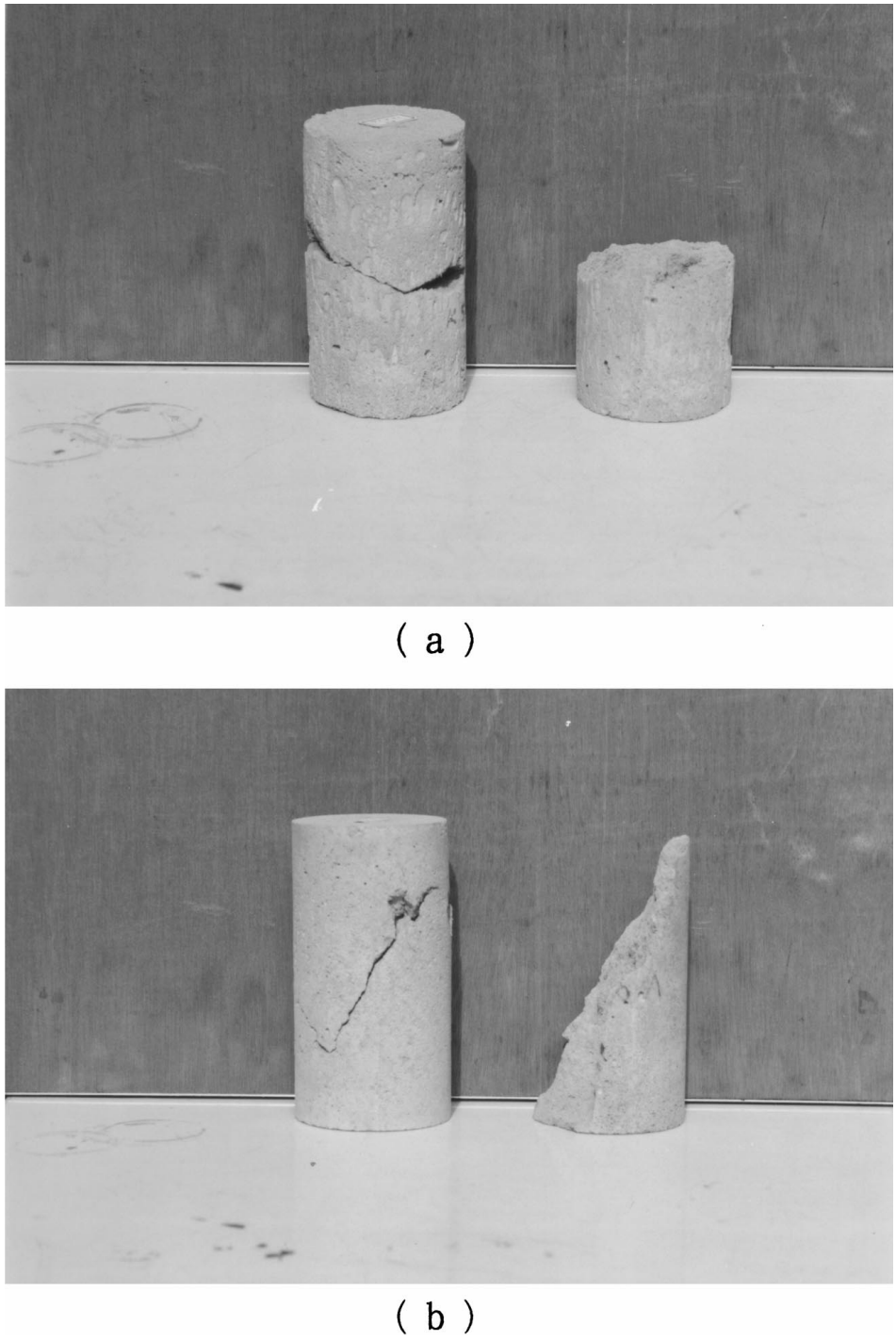

Figure 4 Two failure modes were observed in uniaxial static compression tests for cement foam specimens (a) compressive crushing failure (b) shearing failure.

Here $\Delta\sigma^*$ is in a unit of MPa. The number of cycles to failure for cement foams increases with decreasing normalized cyclic compressive stress range.

In practical applications, most empirical equations describing the number of cycles to failure are expressed in terms of the ratio of cyclic compressive stress range and ultimate compressive strength for cementitious materials. Therefore, Equation 10 can be further written as:

$$\left(\frac{\Delta\sigma^*}{\sigma_u^*}\right) N_f^{*\,0.034} = 0.98 \qquad (11)$$

Equation 9 has been used in the above equation. The exponential constant $a = 0.034$ in Equation 11 for cement foams deviates from 0.043 as presented by Bennett *et al*. [11] for high-strength concrete and from 0.064 as proposed by Hsu [12] for plain concrete. The reason for the deviation might be due to their different composition: pure cement paste with a higher water/cement ratio for solid cell struts in cement foams while a combination of cement paste with a lower water/cement ratio, fine aggregates and coarse aggregates for concrete materials. However, the constant 0.98 on the right-hand side of Equation 11 is close to 1 as expected from the theoretical modelling of Equation 7.

In order to obtain a complete stress-strain hysteresis loop for cycle number up to 10^6, the cyclic compressive stress range is set to be 55% of the ultimate compressive

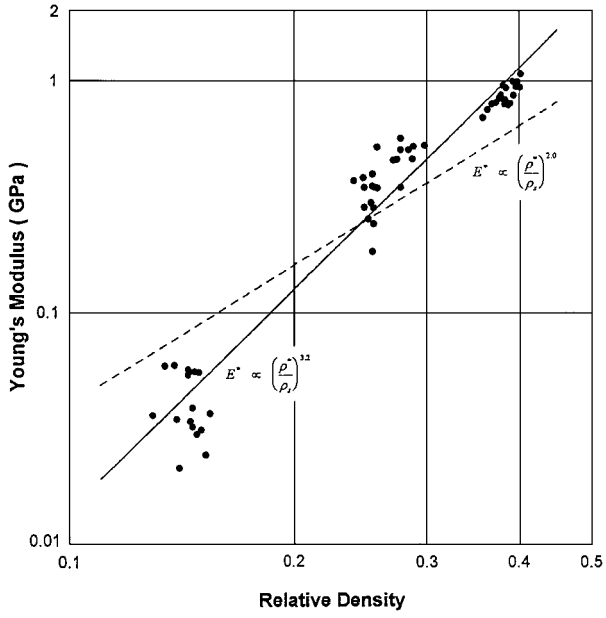

Figure 5 Measured elastic moduli of cement foams are plotted against their relative densities. The elastic modulus of cement foams increases with their relative density and the exponential constant is found to be 3.2.

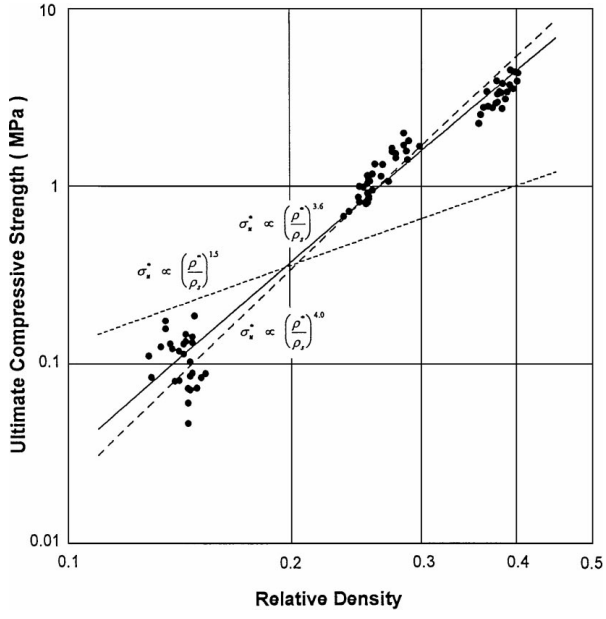

Figure 6 Ultimate compressive strengths of cement foams are plotted against their relative density. The ultimate compressive strength increases with their relative density and the exponential constant is found to be 3.6.

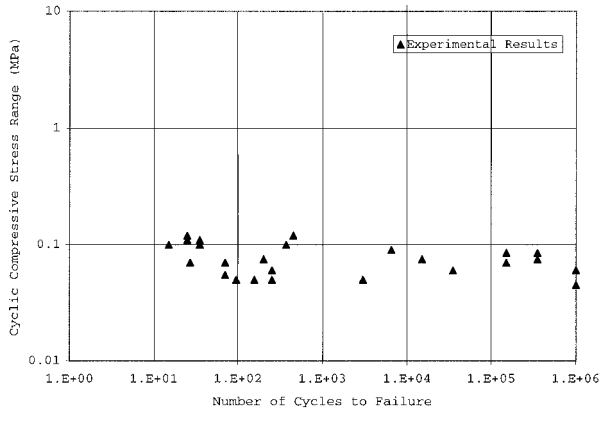

Figure 7 Experimental results for the number of cycles to failure of cement foam specimens with the average relative density of 0.141 subjected to various cyclic compressive stress ranges.

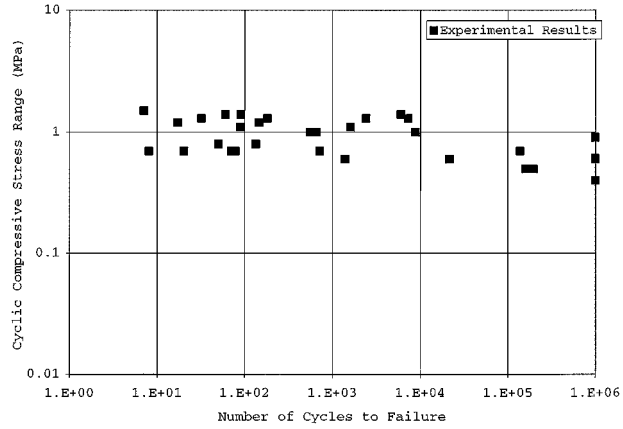

Figure 8 Experimental results for the number of cycles to failure of cement foam specimens with the average relative density of 0.266 subjected to various cyclic compressive stress ranges.

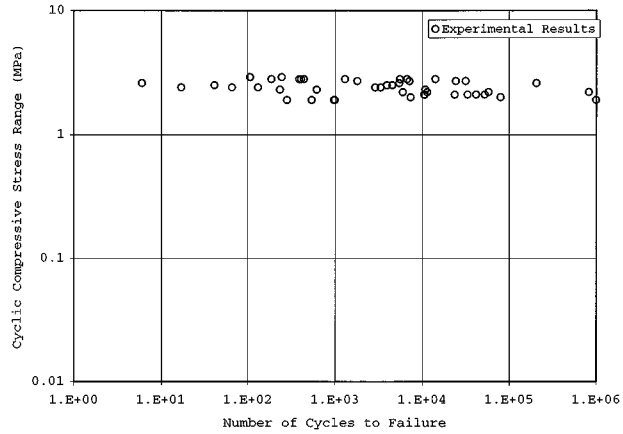

Figure 9 Experimental results for the number of cycles to failure of cement foam specimens with the average relative density of 0.378 subjected to various cyclic compressive stress ranges.

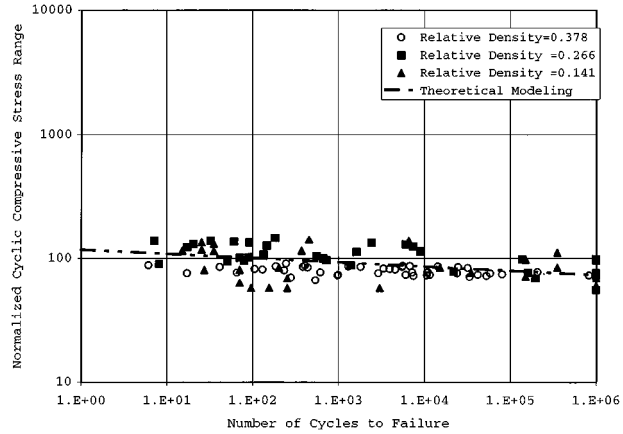

Figure 10 Numbers of cycles to failure for cement foam specimens are plotted against their normalized cyclic compressive stress ranges $\Delta\sigma^*/(\rho^*/\rho_s)^{3.6}$.

strength for cement foams. Fig. 11 shows a typical stress-strain hysteresis loop after various numbers of cycles of loading. It is found that the loss coefficient at each cycle of loading decreases as the number of cycles is increased; the loss coefficient is defined as the ratio of loading and unloading. For most cases, the loss coefficient is roughly 0.30 for the first cycle of loading and is 0.05 after 10^6 cycles of loading. The normalized elastic

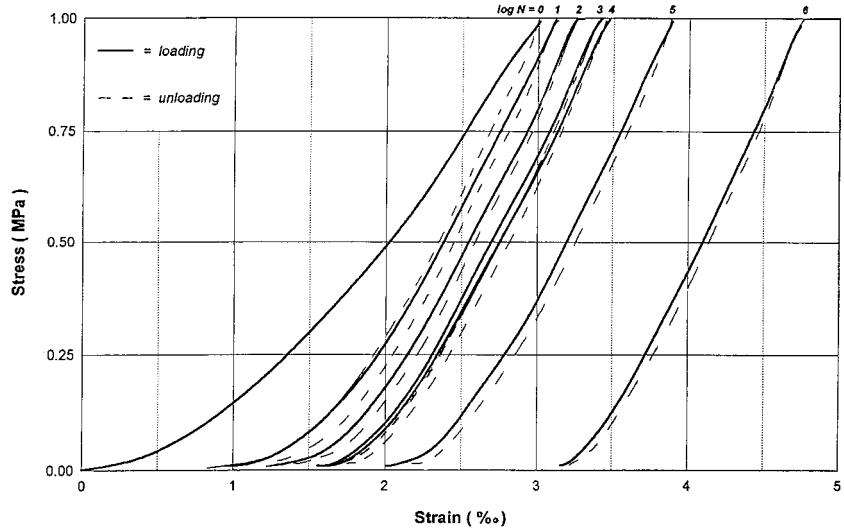

Figure 11 A typical stress-strain hysteresis loop of cement foams after various numbers of cycles of loading.

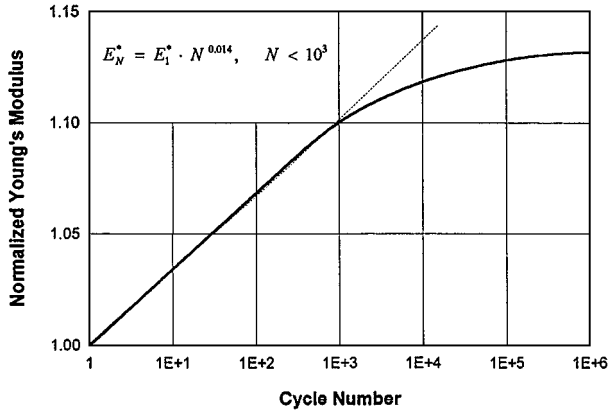

Figure 12 The normalized elastic modulus increases as the number of cycles is increased.

modulus is the elastic modulus taken at the stress level of 0.75 MPa after some cycles of loading, divided by the initial elastic modulus; the normalized elastic modulus increases as the number of cycles is increased as shown in Fig. 12. The cell struts of cement foams are loaded and deformed into a more compact form at the first cycle of loading, and then cement foams become denser after each cycle of loading, giving a higher elastic modulus. The elastic modulus of cement foams, E_N^*, after N cycles of loading (less than 1000) can be estimated from the initial elastic modulus, E_1^*, through the following equation:

$$E_N^* = E_1^* N^{0.014} \quad \text{For } N < 10^3 \qquad (12)$$

After 1000 cycles of loading, some cell-struts fail and touch each other, leading to a gradual increase in elastic modulus.

5. Conclusions

Based on the bending model of individual cell wall in cooperation with dimensional argument analysis, the theoretical expression of fatigue for cement foams in axial compression with a zero stress ratio has been derived. Theoretical results indicate that the number of cycles to failure for cement foams depend on relative density, cyclic compressive stress range and the fatigue parameters of solid cement materials from which they are made. The theoretical expression is compared to the experimental results on cement foams for various relative densities and cyclic compressive stress ranges; the agreement is good. Results suggest that the compressive fatigue can be expressed in terms of the ratio of cyclic compressive stress range and ultimate compressive strength for cement foams. Thus, once the compressive fatigue of any particular relative-density cement foams is known, the fatigue life of other relative-density cement foams can be estimated. However, the effects of loading frequency, stress ratio, water/cement ratio and cell size on fatigue life of cement foams are not studied here and need to be investigated in future research.

Acknowledgement

The financial support of the National Science Council, Taiwan, R.O.C., under contract number NSC 84-2211-E006-018, is gratefully acknowledged.

References

1. F. W. NOBLE and J. LILLEY, *J. Mater. Sci*. **16** (1981) 1801.
2. S. S. YAU and G. MAYER, *Mater. Sci. and Engng*. **78** (1986) 111.
3. K. T. TSAI and M. P. ANSELL, *J. Mater. Sci*. **25** (1990) 865.
4. P. W. BONFIELD and M. P. ANSELL, *ibid*. **26** (1991) 47653.
5. J. S. HUANG and J. Y. LIN, *Acta Mater*. **44** (1996) 289.
6. L. J. GIBSON and M. F. ASHBY, "Cellular Solid: Structures and Properties," 2nd ed. (Cambridge University Press, Cambridge, U.K., 1997).
7. T. D. TONYAN and L. J. GIBSON, *J. Mater. Sci*. **27** (1992) 6371.
8. M. BURMAN and D. ZENKERT, *International J. Fatigue* **19** (1997) 551.
9. *Idem., ibid.* **19** (1997) 563.
10. D. M. ROY and G. D. GOUDA, *J. American Ceramic Soc*. **53** (1973) 549.
11. E. W. BENNETT and S. E. ST J. MUIR, *Mag. of Concrete Research* **19** (1967) 113.
12. T. T. C. HSU, *ACI J*. **78** (1981) 292.

Received 22 June 1999
and accepted 28 February 2000